

## Recent Results from Jefferson Lab

Elton S. Smith <sup>a \*</sup>

<sup>a</sup>Jefferson Lab, Newport News, Va. 23606, USA

Precision measurements of the structure of nucleons and nuclei in the regime of strong interaction QCD are now possible with the availability of high current polarized electron beams, polarized targets, and recoil polarimeters, in conjunction with modern spectrometers and detector instrumentation. We present some recent results from the Jefferson Lab on the charge and current distributions of nucleons and nuclei. We also review measurements which relate physics at small distances to the regime where strong interaction QCD is the relevant theory.

### 1. Introduction

The Continuous Electron Beam Accelerator Facility (CEBAF) at the Thomas Jefferson National Accelerator Facility is devoted to the investigation of the electromagnetic structure of mesons, nucleons, and nuclei using high energy and high duty-cycle electron and photon beams.

CEBAF is a superconducting electron accelerator with an initial maximum energy of 4 GeV and 100 % duty-cycle. Three electron beams with a maximum total current of 200  $\mu\text{A}$  can be used simultaneously for electron scattering experiments in the experimental areas, Halls A, B, and C. The accelerator design concept is based on two parallel superconducting continuous-wave linear accelerators joined by magnetic recirculation arcs. The accelerating structures are five-cell superconducting niobium cavities with a nominal average energy gain of 5 MeV/m. The accelerator performance has met all design goals, achieving 5.5 GeV for physics running, and delivering high quality beams with intensity ratios exceeding  $10^6:1$ . For over a year the electron beam has been produced using a strained GaAs photocathode delivering polarized electrons ( $P_e \geq 75\%$ ) simultaneously to all three halls, completing in excess of 200,000  $\mu\text{A}$ -hours.

Three experimental areas are available for simultaneous experiments, the only restriction being that the beam energies have to be multiples of the single pass energy. The halls contain complementary equipment which cover a wide range of physics problems: Hall A has two high resolution magnetic spectrometers with  $10^{-4}$  momentum resolution in a 10% momentum bite, and a solid angle of 8 msr. Hall B houses the large acceptance spectrometer, CLAS. Hall C uses a combination of a high momentum spectrometer ( $10^{-3}$  momentum resolution, 7 msr solid angle and maximum momentum of 7 GeV/c) and a short orbit spectrometer optimized for the detection of low-energy particles. To date, twelve experiments have been completed (two partially completed) in Hall C, ten

---

\*Supported in part by DOE Contract #DE-AC05-84ER40150.

where the subscripts  $e$  and  $e'$  refer to the incident and scattered electron respectively. The polarization normal to the scattering plane must be zero and can serve as a systematic check. Since the ratio  $G_E^p/G_M^p$  is accessed directly, this experiment has smaller systematic uncertainties than previous experiments at high  $Q^2$  (Figure 1). This experiment confirms the trend of the early data, and extends the  $Q^2$  range to  $3.5 \text{ GeV}^2$ , where the electric form factor has dropped to 60% of the value of the magnetic form factor. The data illustrate beautifully the power of polarization in electromagnetic interactions. The experiment will be continued to higher momentum transfer in the year 2000 [12].

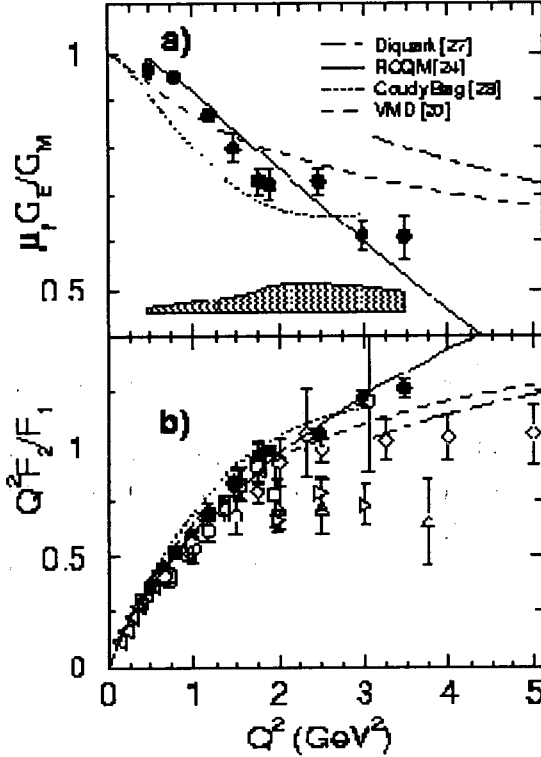


Figure 1. (a) The ratio  $\mu_p G_E^p/G_M^p$  from this experiment, compared with theoretical calculations. (b) The ratio  $Q^2 F_2^p/F_1^p$  for the same data, compared to the same theoretical models as in (a) and world data.

## 2.2. The $\gamma N \Delta$ transition.

The lowest excitation of the nucleon is the  $\Delta(1232)$  ground state. The electromagnetic excitation is due predominantly to a quark spin flip corresponding to a magnetic dipole transition. The interest today is in measuring the small electric and scalar quadrupole transitions which are predicted to be sensitive to the possible deformation of the nucleon or the  $\Delta(1232)$  [13]. Contributions at the few percent level may come from the pion cloud at large distances, and gluon exchange at small distances. An intriguing prediction

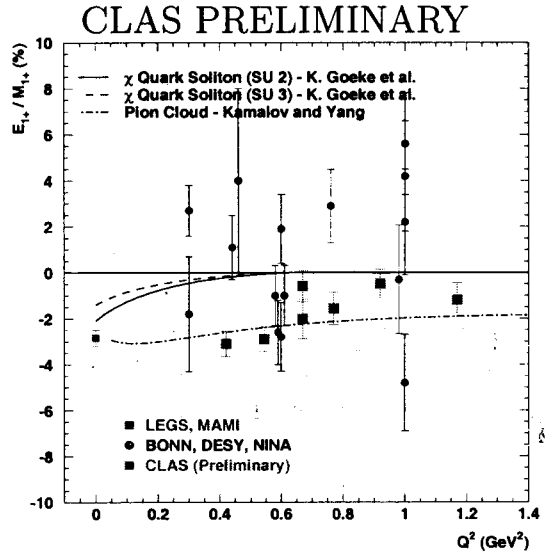


Figure 2. Ratio of  $E_{1+}/M_{1+}$  measured using exclusive production of  $ep \rightarrow ep\pi^0$  and the CLAS detector.

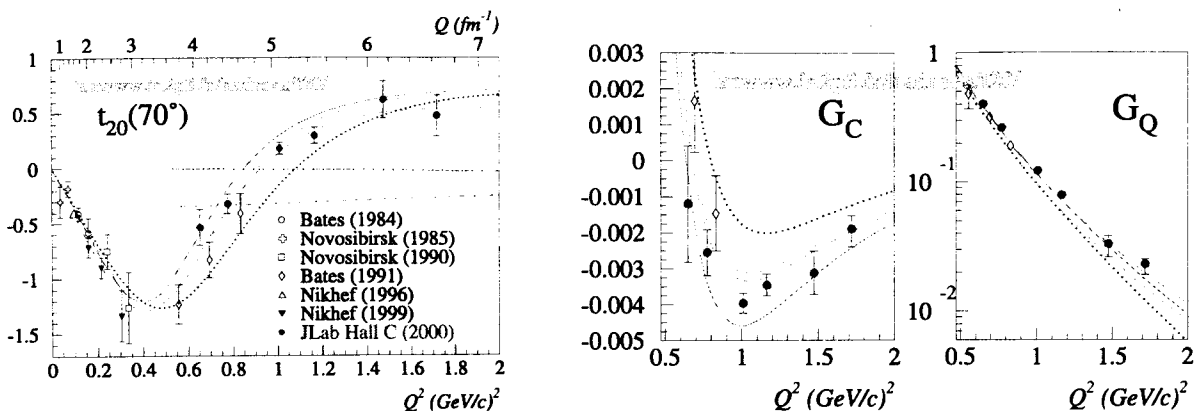


Figure 3.  $t_{20}$  at  $\theta_e=70^\circ$  and monopole ( $G_C$ ) and quadrupole ( $G_Q$ ) charge form factors of the deuteron compared to theoretical predictions; dotted line (NRIA) and full line (NRIA+MEC+RC); relativistic models with dashed line and and long dashed line; pQCD calculations with dashed- dotted line and long dashed-dotted line.

There is significant interest in the high  $Q^2$  behavior of these form factors because they probe the short distance behavior of the nucleon-nucleon interaction. A large variety of models have been developed to describe the form factors for a wide range in distance scales, from hadronic models to descriptions within the framework of perturbative QCD. Nevertheless, the data are described by modern hadronic models. Even the approach to scaling can be understood within these models, so that quark-gluon degrees of freedom need not be invoked to describe the data even at the highest momentum transfers.

#### 4. The Nucleon Spin Structure - from Small to Large Distances

The internal spin structure of the nucleon has been of central interest ever since the EMC experiment found that at small distances the quarks carry only a fraction of the nucleon spin. Going from small to large distances the quarks get dressed with gluons and  $q\bar{q}$  pairs and acquire more and more of the nucleon spin. How is this process evolving with the distance scale? At the two extreme kinematic regions we have two fundamental sum rules: the Bjorken sum rule (Bj-SR) which holds in the asymptotic limit, and is usually written for the proton-neutron difference as

$$\Gamma_1^{pn}(Q^2) = \lim_{Q^2 \rightarrow \infty} \int g_1^p(x, Q^2) dx - \int g_1^n(x, Q^2) dx = \frac{g_A}{6}. \quad (4)$$

At the finite  $Q^2$  where experiments are performed, QCD corrections have been calculated, and there is good agreement between theory and experiment at  $Q^2 > 2 \text{ GeV}^2$ . At the other end, at  $Q^2 = 0$ , the Gerasimov Drell-Hearn sum rule (GDH-SR) is expected to hold:

$$I_{GDH} = \frac{M^2}{8\pi^2\alpha} \int \frac{\sigma_{1/2}(\nu) - \sigma_{3/2}(\nu)}{\nu} d\nu = -\frac{1}{4}\kappa^2. \quad (5)$$

The integral for the difference in helicity 1/2 and helicity 3/2 total absorption cross sections is taken over the entire inelastic energy regime. The quantity  $\kappa$  is the anomalous

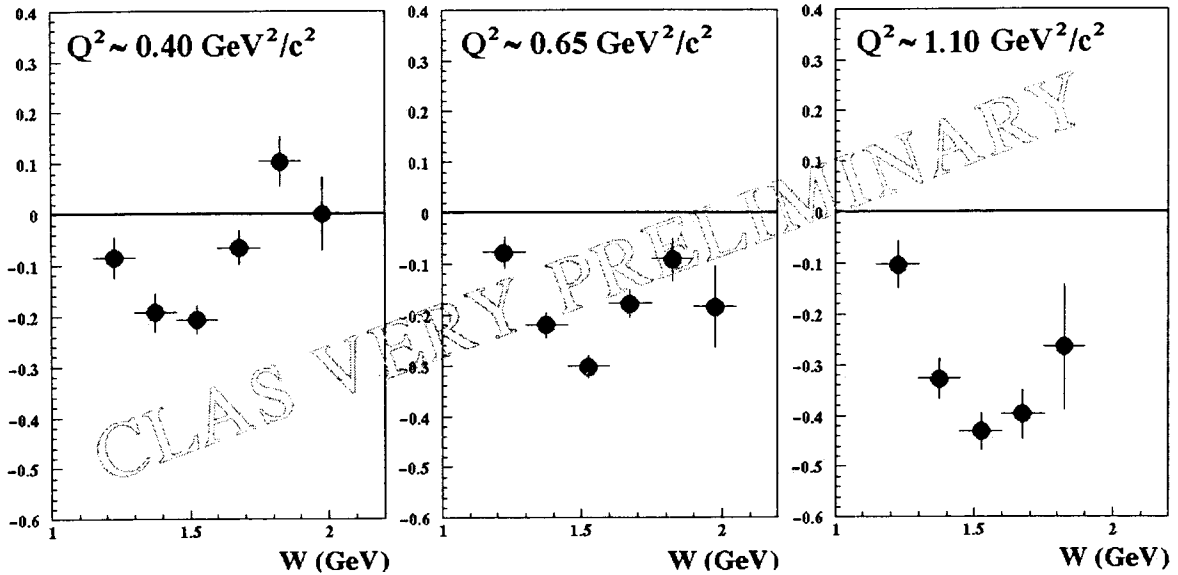


Figure 4. Double spin asymmetry measured using the CLAS detector for the exclusive channel  $\vec{e}\vec{p} \rightarrow e n \pi^+$  at three values of  $Q^2$ .

effects. This behavior may be understood as the probability for scattering off free quarks at large  $Q^2$  is the same as scattering off constituent quarks at lower energies. Until recently, this intriguing observation was little utilized. A new inclusive ep scattering experiment at JLAB [35] helped rekindle the interest in this aspect of hadron physics by testing the limits of this conjecture resonance by resonance (local duality) and at very small  $Q^2$ . Figure 6 shows that the structure functions  $F_2$  for hydrogen and deuterium in the resonance region oscillate around the DIS curve (NMC). The measurements of  $F_2$  in the resonance region and small  $Q^2$  tend toward zero, similar to the valence quark distributions in the deep inelastic region. This can be understood by noting that the distribution of perturbative sea quarks is expected to be small at  $Q^2 = 0$ , and the behavior of non-perturbative sea quarks has valence-like behavior in Regge phenomenology [36].

## 6. Photoproduction at large momentum transfer

A significant fraction of the program at Jefferson Lab has been devoted to experiments with photon beams which we have not detailed here due to the lack of space. The interest in these reactions stems from the fact that they allow relatively high momentum transfer to the constituents at modest photon energies. An example of such experiments is the two-body photo-disintegration of the deuteron ( $\gamma d \rightarrow pn$ ), which has been used to investigate constituent-counting rules and the transition from meson-nucleon degrees of freedom to quark-gluon degrees for freedom [37]. Another experiment has recently been completed with CLAS to measure the photo-production of  $\phi$ -mesons for momentum transfers up to  $4.5 \text{ GeV}^2$ . The data support models that decompose the Pomeron into its simplest components, namely two gluons which couple to quarks inside the  $\phi$  and the proton [38].

8. B. Anderson, S. Kowalski, R. Madey *et.al.*, JLAB experiment E-93-038
9. D. Day *et.al.*, JLAB experiment E-93-026
10. For a previous review of Jlab results, see V. Burkert, nucl-th/9912009 and references therein
11. M.K. Jones *et.al.*, Phys. Rev. Lett. 84, 1398 (2000)
12. E. Brash, M.K. Jones, C. Perdrisat and V. Punjabi *et.al.*, JLAB experiment E-99-007
13. V. Frolov *et al.*, Phys. Rev. Lett. 82, 45 (1999)
14. C.E. Carlson, Phys. Rev. D34, 2704 (1986)
15. L.C. Smith *et.al.*, to appear in the proceedings of the Jlab Nstar2000 Workshop, Feb 16-19, 2000
16. L.C. Alexa *et.al.*, Phys. Rev. Lett. **82**, 1374 (1999)
17. D. Abbott *et.al.*, Phys. Rev. Lett. **82**, 1379 (1999)
18. E. Beise, S. Kox *et al.*, Jlab experiment E94-018
19. The JLAB t20 collaboration: D. Abbott *et al.*, nucl-ex/0001006 (2000)
20. X. Ji, J. Osborne, hep-ph/9905010 (1999)
21. X. Ji, C.W. Kao, and J. Osborne, hep-ph/9910256
22. V. Burkert and B. Ioffe, Phys. Lett. B296, 223 (1992)
23. V. Burkert and B. Ioffe, J.Exp.Theo.Phys. 78, 619 (1994)
24. J. Soffer and O. Teryaev, Phys. Rev.Lett. 70, 3373 (1993)
25. K. Abe *et al.*, Phys. Rev. D58, 2003 (1998)
26. V. Burkert and Zh. Li, Phys. Rev. D47, 46 (1993)
27. W.X. Ma, D.H. Lu, A.W. Thomas, Z.P. Li, Nucl. Phys. A635 497 (1998)
28. V. Burkert, nucl-th/0004001 (2000)
29. V. Burkert, D. Crabb, R. Minehart *et al.*, JLAB experiment E-91-023
30. S. Kuhn, M. Taiuti *et al.*, JLAB experiment E93-009
31. Z. Meziani, *et al.*, JLAB experiment E94-010
32. K. Ackerstaff *et al.*, Phys. Letts. B444, 531 (1998)
33. R. DeVita *et al.*, to appear in the proceedings of the Jlab Nstar2000 Workshop, Feb 16-19, 2000
34. E.D. Bloom and F.J. Gilman, Phys. Rev. D4, 2901 (1970)
35. I. Niculescu *et al.*, accepted for publication in Phys. Rev. Lett.
36. W. Melnitchouk, contribution to this workshop
37. C. Bochna *et al.*, Phys. Rev. Lett. 81, 4576 (1998)
38. M. Battaglieri, contribution to this workshop